SPECTROSCOPIC STUDIES OF INHIBITED OPPOSED FLOW PROPANE/AIR FLAMES

R.R. SKAGGS, R.G. DANIEL, A.W. MIZIOLEK, AND K.L. McNESBY
U.S. Army Research Laboratory
Aberdeen Proving Ground, MD 21005

Introduction

Fire protection on military platforms, including ground fighting vehicles, is being challenged by the impending loss of the ubiquitous fire fighting agent halon 1301 (CF_3Br) due to environmental concerns related to the destruction of the stratospheric ozone layer. Replacement fire extinguishment agents need to be found that will satisfy numerous criteria including: fast fire suppression, minimum production of toxic gases when used, low toxicity, compatibility with storage materials and environmental friendliness.

The U.S. Army's search for halon replacement agents has largely involved an empirical approach of testing and evaluation of commercially available compounds/systems. An alternative approach is to study the fundamental physical and chemical mechanisms responsible for flame inhibition with the hope that such studies will uncover differences in the flame inhibition mechanisms which will lead to new chemicals for further consideration and testing. To this end, we have recently initiated planar laser induced fluorescence (PLIF) measurements of the OH radical species as flame extinction was approached in a non-premixed, atmospheric pressure, opposed flow propane/air flame inhibited by halon 1301 [CF_3Br], N_2, $Fe(CO)_5$, FM-200 [C_3F_7H], FE-36 [$C_3F_6H_2$], DMMP [$CH_3P(O)(OCH_3)_2$], PN [$P_3N_3F_6$]. Presented here are preliminary results from this study of compounds which represent distinctly different chemical families in order to understand the differences in each agent's inhibition mechanism.

Background

Chemical inhibition in a flame arises from the lowering of the radical concentrations due to scavenging reactions. In general, effective inhibition mechanisms contain two types of reactions: a) radical scavenging reactions, and b) reactions regenerating inhibitor species that participate in the inhibition cycle. As an example, for CF_3Br inhibition a free bromine from decomposed CF_3Br forms HBr which chemically reacts with hydrogen atom and reduces hydrogen's concentration. The consequence of hydrogen recombination is the overall available radical concentrations (H, O, OH) and the rate of chain-branching reactions are reduced [1,2,3,4] while regeneration of HBr and Br_2 occurs restarting the inhibition cycle.

The chemicals $Fe(CO)_5$, DMMP, and PN investigated in our laboratory flame system were chosen based on a comprehensive evaluation [5] of fire inhibitors that are more effective than CF_3Br. The inhibition mechanisms for $Fe(CO)_5$, DMMP, and PN are believed to be generally similar to the HBr mechanism. For these postulated mechanisms, each agent decomposes during combustion into inhibition cycle scavenging species, e.g. FeO, FeOH, $Fe(OH)_2$ for $Fe(CO)_5$ addition, [6] and HOPO and $HOPO_2$ for DMMP and PN addition [7]. In the reaction zone of flames, these scavenging species proceed to behave much like HBr in scavenging hydrogen atoms. FM-200 and FE-36 were studied here due to their popularity as candidate halon replacement agents.

Flame inhibition by CF_3Br is not completely due to chemical reactions, where previous studies [8] have shown that at least 20 % of its inhibition capability is caused by physical properties, i.e. heat capacity. In order to understand a chemical's inhibition mechanism in terms of physical and/or chemical contributions, both N_2 and CF_3Br are included in this study. That is, N_2 represents the upper boundary for physical influence on flame inhibition since it has no chemical inhibition capabilities, while CF_3Br with its known physical and chemical contributions offers a good intermediate point with which to compare and contrast the other agents studied.

Experimental

OH PLIF imaging measurements were made using the arrangement presented in **Figure 1.** The opposed flow burner apparatus is located inside a stainless steel hood to contain any toxic fumes that are exhausted from the burner. All flames analyzed in this work were studied at atmospheric pressure and consisted of 7.0 L/min synthetic air (79% N_2 + 21% O_2) flowing from the lower duct, and 5.6 L/min of propane flowing from the upper duct. The oxidizer and fuel ducts are separated a distance of 1.2 cm and the duct diameter is 2.54 cm. Based on the flow conditions and duct separation, the luminous flame zone is located on the oxidizer side of the stagnation plane and

the global strain rate is 72.51 sec^{-1}. For all studies presented here, the inhibitor agents are added to the oxidizer flow in gaseous form at room temperature with the exception of $Fe(CO)_5$ which was cooled to 11°C and DMMP which was heated to 70°C. Opposed flow burners have been used for some time to study the capabilities of an inhibitor agent because a global parameter, the extinction strain rate [9], can be determined which describes the flame's strength at extinction [10,11,12,13]. The extinction strain rate is useful because a decreased value demonstrates an inhibitor's efficiency. PLIF measurements of radical concentrations (O, H, OH) are complimentary to the extinction strain rate because the measurements illustrate an inhibitor's influence on the radical concentration profiles in the flame zone which indicates if the flame's radical chemistry is being perturbed by agent addition. OH is monitored in the flames studied here because it is relatively simple to measure and it is a good indicator of the overall radical pool concentration, even though H, O, and OH have been found to not be fully equilibrated in diffusion flames [14].

Planar laser induced fluorescence images were measured using a Lambda Physik excimer/dye laser system. This system consists of a Lambda Physik Compex 102 XeCl excimer laser, a Scanmate 2 dye laser (Coumarin 153) and a Second Harmonic Generator (SHG). The fundamental output of the dye laser (540 nm wavelength) was frequency doubled in the SHG unit with a BBO crystal to approximately 281 nm. The UV laser radiation was tuned to the peak of the $R_2(9.5)$ transition at 281.8 nm ((1,0) $A^2\Sigma^+ \leftarrow X^2\Pi$) [15,16,17]. This transition was chosen because it is less temperature dependent than other nearby transitions [18]. The UV light output of the SHG unit enters an optical train where the beam is turned 90°, apertured by a sub mm iris, projected through a cylindrical plano convex lens to form the UV beam into a vertical sheet. To create a uniform sheet width, the sheet is apertured with 0.5 mm vertical slits as it is projected toward the center of the burner. The UV sheet is apertured just before the burner to produce a vertically uniform intensity that is 1.2 cm in height allowing passage through the entire burner flow field. Laser induced fluorescence from OH passes through a band pass filter centered at 312 nm with an 11 nm bandwidth and is detected with a Princeton Instruments ICCD camera (Model 120) coupled with a Nikon UV lens located at 90° with respect to the UV sheet. The ICCD camera, which has an active area of 384 x 576 pixels, has a field of view with this optical arrangement of approximately 33 cm^2 and each image recorded was acquired with 25 total accumulations on the camera.

Results

Figure 2 presents two representative two-dimensional images of OH fluorescence for an uninhibited propane/air flame and for a propane/air flame to which CF_3Br was added (1.5 % by volume). Both images, which are uncorrected for laser energy fluctuations and local quenching rates, illustrate the presence of two luminous zones as the UV sheet passes through the flame. The lower, thicker zone is the fluorescence from the OH transition while the upper zone is the broadband fluorescence due to derivative fuel species such as polycyclic aromatic hydrocarbons. To construct a spatially resolved OH LIF profile from an image, as shown on the right hand side of **Figure 2**, the pixel intensity corresponding to a given height between the fuel and oxidizer ducts (spatial resolution approximately 0.149 mm/pixel) was summed and averaged over a 1 mm width. The two-dimensional images and LIF profiles illustrate that addition of CF_3Br to the propane flame causes a decrease in the OH fluorescence signal while the broadband fluorescence appears to increase just slightly. Similar results have been seen previously for CF_3Br addition to hydrocarbon diffusion flames [19,20]. Each OH intensity profile is fit to a gaussian function to determine the area under the profile curve. The profile area provides a general indicator of the OH behavior for a given flame condition because it accounts for changes in both the profile width and the profile's position relative to the flow ducts as inhibitor concentrations increase in the flame. PLIF images similar to those in **Figure 2** were acquired and analyzed for each agent studied.

Figure 3 plots the results of the measured OH profile areas versus each inhibitor agent's concentration as the flames were stepped towards extinction. It should be noted that the reported areas are averaged over three or more separate extinction experiments, where the data for each experiment are normalized to the OH profile area measured in the uninhibited flame acquired prior to each extinction experiment to account for changes in burner and camera conditions. The data here indicate that there are both physical and chemical modes of inhibition being observed for the agents studied. N_2 has the least impact on OH with respect to the other agents studied while the two fluorinated propanes (FM-200 and FE-36) show initially small declines in OH, but more rapid decreases as extinction is approached. For the other agents studied (PN, CF_3Br, DMMP, and $Fe(CO)_5$), the addition of these

inhibitors show more dramatic decreases in the measured OH values. Finally, **Table 1** lists the observed extinction inhibitor concentrations in the air stream for each agent studied here and their estimated uncertainties.

Table 1: Inhibitor concentrations (% volume) and uncertainty (± % volume) at flame extinction

Inhibitor Agent	N_2	FE-36	FM-200	PN	CF_3Br	$Fe(CO)_5$	DMMP
Extinction Concentration	35.9	10.6	9.1	6	4.4	0.5	0.4
Estimated Uncertainty	12.3	1.56	1.88	0.63	1.47	0.10	0.03

It should be noted that the extinction concentration for CF_3Br is very similar to values found for analogous flames and cup burners [20], while the fluorinated propanes are slightly higher than their reported cup burner values [21]. Unfortunately there are no cup burner values reported for DMMP. Recent cup burner experiments for PN [22] indicate the value observed in our experiments is a factor of 6 greater than the literature value. At this time there is no explanation for the PN extinction concentration discrepancy and future experiments will address this issue in more detail.

Conclusions

The results presented here show for the first time changes in OH as extinction is approached in an atmospheric pressure, non-premixed, propane/air flame. The OH profiles illustrate that N_2, FE-36, and FM-200, with smaller changes in OH relative to CF_3Br, exhibit chemical inhibition capacities less than CF_3Br. On the contrary, DMMP and $Fe(CO)_5$ demonstrate chemical inhibition capabilities greater than CF_3Br with their larger changes in OH. For the inhibitors studied, agent concentrations at extinction support these observations with a CF_3Br concentration of 4.4 % (by volume) compared to N_2 with a concentration of 35.9 % and DMMP and $Fe(CO)_5$ each having concentrations less than 1 %.

Figures

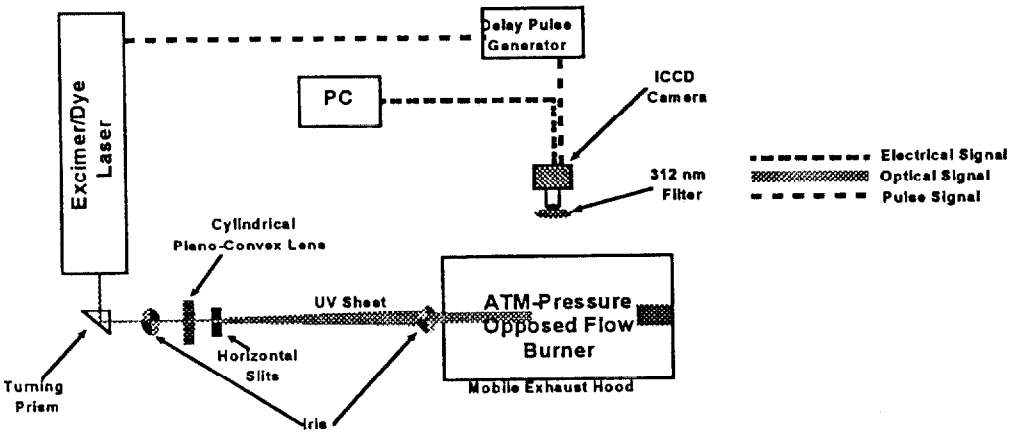

Figure 1: Schematic diagram of the experimental apparatus.

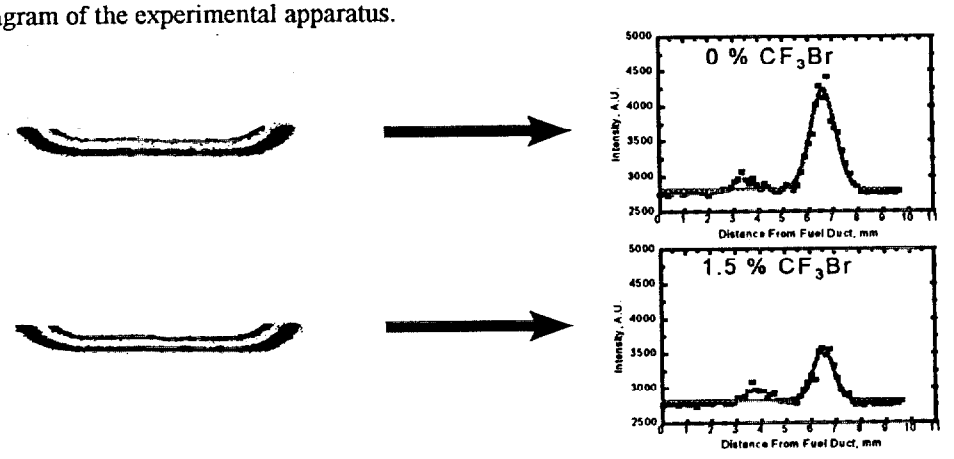

Figure 2: Representative PLIF images and the corresponding OH intensity profiles from an opposed flow propane/air flame seeded with 0 % (by volume) CF_3Br and 1.5 % (by volume) CF_3Br. Note the orientation of the PLIF images with respect to the burner system places the fuel and air ducts at the top and bottom of the images respectively.

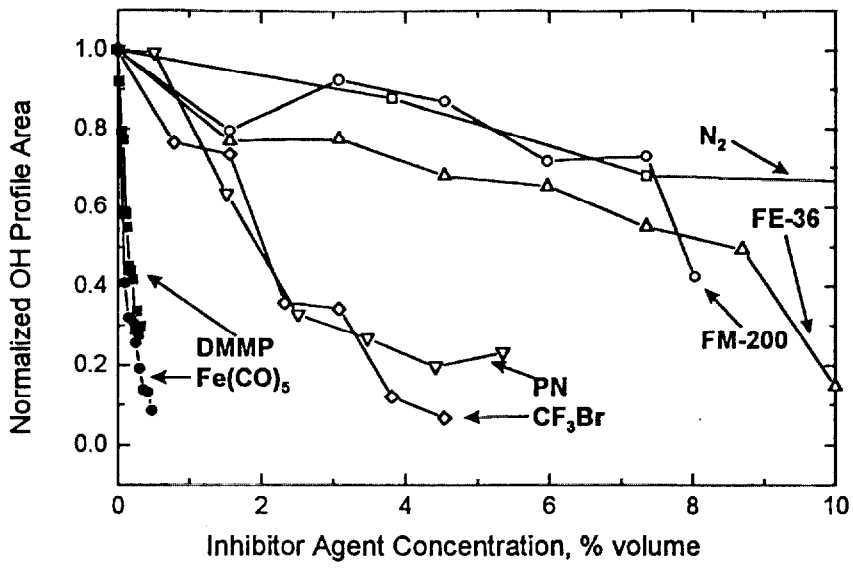

Figure 3: Normalized OH LIF profile areas versus agent delivery concentrations. The (□) are the N_2 data, the (○) are the FM-200 data , the (△) are the FE-36 data, the (▽) are the PN data, the (◇) are the CF_3Br data, the (■) is the DMMP data and the (●) are the $Fe(CO)_5$ data.

Acknowledgments

The authors would like to thank Anthony Hamins (NIST) for burner fabrication and Valeri Babushok (NIST) for insightful suggestions and comments concerning experiments and results. This work was supported by the Next Generation Fire Suppression Technology Program under the auspices of the U.S. Army TACOM (Steve McCormick). Finally R. Skaggs would like to acknowledge financial support from the Army Research Laboratory through an American Society for Engineering Education Postdoctoral Fellowship.

References

1. Dixon-Lewis, G., Simpson, R.J., *Sixteenth Symposium (International) on Combustion*, The Combustion Institute, Pittsburgh, 1976, p.1111.
2. Westbrook, C.K. *Combust. Sci. Technol.* 23: 191 (1980).
3. Westbrook, C.K. *Nineteenth Symposium (International) on Combustion*, The Combustion Institute, Pittsburgh, 1982, p.127.
4. Westbrook, C.K. *Combust. Sci. Technol.* 34: 201 (1983).
5. Babushok, V., Tsang, W. *Chemical and Physical Processes in Combustion: Proceedings of Fall Technical Meeting of the Eastern States Section of the Combustion Institute*, 1997, p.79.
6. Rumminger, M.D., Reinelt, D., Babushok, V.I., and Linteris, G.T., 116: 207 (1999).
7. MacDonald, M.A. Jayaweera, T.M. Fisher, E.M., Gouldin, F.C. *Combust. Flame* 116: 166 (1999).
8. Noto, T., Babushok, V., Burgess, D.R., Hamins, A., Tsang, W., Miziolek, A., *Twenty-Sixth Symposium (International) on Combustion*, 1996, p.1377.
9. Seshadri, K. and Williams, F., *Int. J. Heat and Mass Tarnsfer* 21:251 (1978).
10. Potter, A.E., Heimel, S., and Butler, J.N., *Eighth Symposium (International) on Combustion*, The Combustion Institute, Pittsburgh, 1962, p.1027.
11. Carrier, G.F., Fendell, F.E., and Marble, F.E., SIAM *J. Appl Math.* 28: 463-500 (1975)
12. Linan, A. *Acta Astronaut* 1: 1007 (1974).
13. Williams, F.A. *Fire Saf. J.* 3:163 (1981)
14. Smyth, K.C., Tjossem, P.J.H., Hamins, A., and Miller, J.H., *Combust. Flame* 79: 366 (1990).
15. Chidsey, I.L., and Crosley, D.R., *J Quant. Spectrosc. Radiat. Transf*, 23: 187 (1980)
16. Dieke, G.H., and Croswhite, H.M., *J Quant. Spectrosc. Radiat. Transf.* 2: 97 (1962).
17. Kotlar, A., Private Communication (1998).
18. Eckbreth, A.C., in *Laser Diagnostics for Combustion Temperatures and Species*, Abacus Press, Cambridege Mass., (1988).
19. Masri, A.R., Dally, B.B., Barlow, R.S., and Carter, C.D., *Combust. Sci. Technol.* 113-114: 17 (1996).
20. Smyth, K.C., and Everest, D., *Twenty-Sixth Symposium (International) on Combustion*, 1996, p.1385.
21. *Cup-Burner Flame Extinguishment Concentrations*, NMERI Report http://www.nmeri.unm-cget, 1998.
22. Kaizerman, J.A., and Tapscott, R.E. *Advanced Streaming Agent Development, Volume III: Phosphorus Compounds*, New Mexico Engineering Research Institute, Report No. NMERI 96/5/32540, 1996.